

# Top Flavoured Dark Matter in Dark Minimal Flavour Violation

GK Plenary Workshop, Freudenstadt

Monika Blanke, **Simon Kast** | September 26, 2016

KARLSRUHE INSTITUTE OF TECHNOLOGY



- 1 Introduction
  - Simplified Models
  - Dark Minimal Flavour Violation
- 2 Phenomenology
  - Detector Constraints
  - Flavour Constraints
  - Relic Abundance Constraints
  - Direct Detection Constraints
  - Combined Analysis
- 3 Summary and Outlook

- Presence of dark matter ( $\Omega_{DM} \approx 27\%$ ) demands extension of Standard Model (SM).  
→ What can we do to find the right extension?
- One extreme: full theory extension of SM (e.g. SUSY).
- Other extreme: effective field theory (EFT) approach.
- The middle way: simplified models.
- Advantage of simplified models: study specific interactions with limited number of parameters.

# The Flavour Gate to Dark Matter

Assume an analogy to the SM fermions  $\rightarrow$  dark flavour triplet  $\chi_i$ .

Assume an analogy to the SM fermions  $\rightarrow$  dark flavour triplet  $\chi_i$ .

Flavoured dark matter coupling to SM right-handed up quark triplet:

$$\mathcal{L}_{\text{NP,int}} = -\lambda_{ij} \bar{U}_{Ri} \chi_j \phi + h.c.$$

- DM flavour triplet  $\chi_j$ , Dirac fermion, SM gauge singlet.
- Heavy scalar mediator  $\phi$ , carrying colour and hypercharge.
- Lagrangian has unbroken  $\mathbb{Z}_3$  symmetry and hence yields stability of DM  $\chi$  (for  $m_\phi > m_\chi$ ).

# Dark Minimal Flavour Violation

[Agrawal, Blanke, Gemmler '14]

Flavour symmetry

$$U(3)_u \times U(3)_d \times U(3)_q \times U(3)_\chi$$

is only broken by SM Yukawa couplings and the DM-quark coupling  $\lambda_{ij}$  (Dark Minimal Flavour Violation).

⇒ only DM mass splitting originates from RG running:

$$m_{ij} = m_\chi (\mathbb{1} + \eta \lambda^\dagger \lambda + \dots)_{ij}.$$

- $\eta$  depends on the full theory → has to be a parameter of the simplified model.
- Flavour with lowest mass is our DM candidate.  
→ we choose the “top-flavour”. [Kilic, Klimek, Yu '15]

After using all the symmetries at our disposal,  $\lambda$  has 9 parameters left and can be parametrized as:

$$\lambda = U_{23}^\lambda U_{13}^\lambda U_{12}^\lambda D_\lambda$$

- $D_\lambda$  is a real diagonal matrix  $D_\lambda = \text{diag}(D_{\lambda,11}, D_{\lambda,22}, D_{\lambda,33})$ .
- $U_{ij}^\lambda$  are unitary matrices with mixing angles  $\Theta_{ij}$  and phases  $\delta_{ij}$ .

$\Rightarrow$  new source of flavour and CP violation

# Constraints from SUSY Searches at LHC

Constraints from SUSY searches ( $t\bar{t}$  or dijet final states)

[ATLAS collaboration '14]

Study  $pp \rightarrow \phi\bar{\phi} \rightarrow q\bar{q}\chi\bar{\chi}$

- Production either through  $g\phi\bar{\phi}$  or NP interaction (coupling-dependent).
- Decay either to top or jet (+  $\cancel{E}_T$ ).

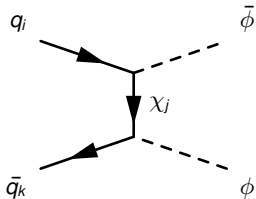


Figure : NP interaction production channel.

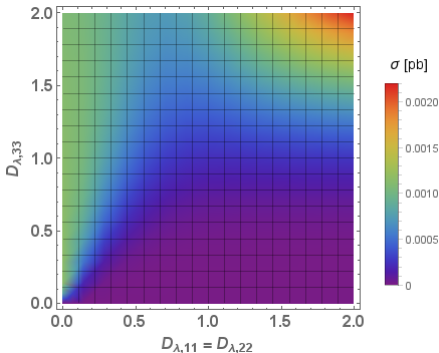
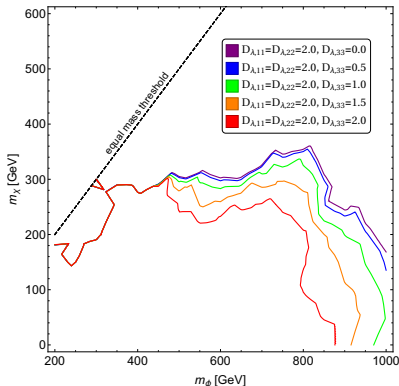


Figure : Cross section for  $t\bar{t}$  final state, mixing angles set to zero.



[ATLAS collaboration '14]



**Figure** : Exclusion plot for dijet final state, mixing angles set to zero.

- The phenomenologically interesting region is  $m_\chi \leq 1$  TeV.
- Too large couplings  $D_{\lambda,ii}$  would exclude nearly all of parameter space.
- Most serious constraints are given by searches for dijet final state.

⇒ Safe parameter space:

$$m_\phi \geq 850 \text{ GeV}$$

$$2.0 \geq D_{\lambda,33} > D_{\lambda,22}, D_{\lambda,11}$$

⇒ Also save with mixings allowed.

# Flavour Constraints from Neutral Meson Mixing

[UTfit collaboration '14]

- No mesons with top quark are possible, the only constraints come from D mesons.  
⇒ not too strong
- The NP contribution has to be smaller than experimental bounds.  
⇒ constraints on mixing angles, mostly  $\Theta_{12}$

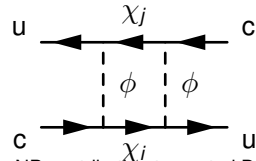


**Figure :** NP contribution to neutral D meson mixing.

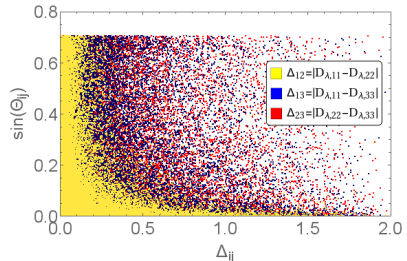


**Figure :** Valid mixing angles for different coupling splittings.  $m_\phi = 850$  GeV,  $m_\chi = 250$  GeV.

# DM Constraints from Observed Relic Abundance

[Steigman, Dasgupta, Beacom '12]

- Assume DM abundance as a thermal relic.
- Depending on mass splitting several freeze out scenarios are possible.
- If DM mass is below top mass several channels drop out.  
⇒ different impact on parameters
- Co-annihilation has to be just as large as to produce the correct relic density.  
⇒ cuts out valid area for  $D_{\lambda,ii}$  depending on  $m_\phi$  and  $m_\chi$
- Lower bounds on DM mass depending on mediator mass.
- Depending on  $\eta$  an upper DM bound arises in single flavour freeze out scenarios.

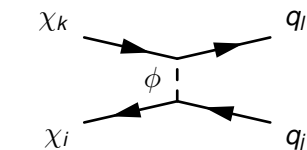


Figure : Coannihilation of DM flavours.

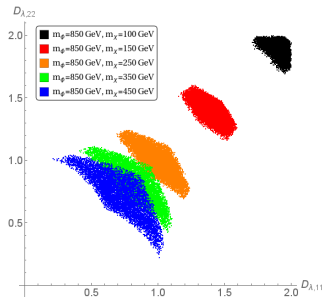


Figure : Valid points in quasi degenerate freeze out scenario.

# DM Bounds from Direct Detection Experiments

[LUX collaboration '16]

- Many contributions to total WIMP-nucleon cross section, only Z-penguin with neutron is negative.  
⇒ saves the day
- Tree level and neutron Z-penguin have to nearly cancel each other.  
⇒ serious constraints on  $\Theta_{13}$
- For too large couplings the cancellation is no longer possible → excluded.
- Top flavoured DM is the natural choice.

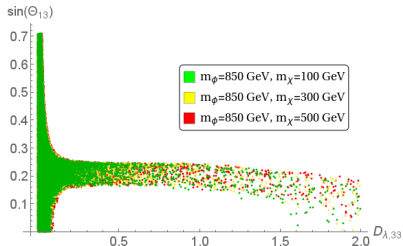


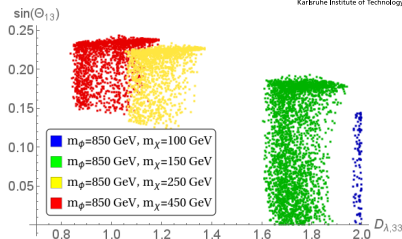
Figure : Valid mixing angle  $\Theta_{13}$  vs  $D_{\lambda,33}$ .



Figure : Cancellation of tree level and neutron Z-penguin contributions (symbolic).

# Combined Analysis of Constraints

- A combination of relic abundance and direct detection constraints confine  $\Theta_{13}$  to a narrow interval around the “perfect” cancellation point.
- The lower and upper bounds on the DM mass become more serious, since the parameters do not only have to fulfill relic abundance constraints.
- The combined analysis clearly prefers top flavoured DM.



**Figure :** Valid points in  $\Theta_{13}$ - $D_{\lambda,33}$ -plane (QDF).

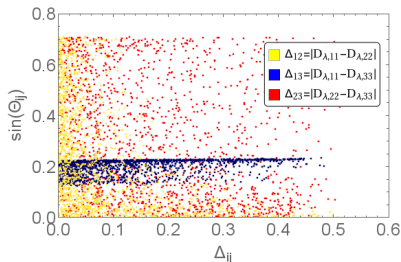


**Figure :** Valid points for  $m_\phi = 850$  GeV and  $m_\chi = 250$  GeV (QDF).

- A simplified model of flavoured DM coupled to SM right-handed up quark triplet. Coupling is general following the concept of DMFV.
- Assuming  $m_\chi < 1$  TeV (phenomenologically interesting area).
- With this mass the RA constraints demand high  $D_{\lambda,ii}$  for high mediator mass  $m_\phi$ .
- High couplings prevent the necessary cancellation in WIMP-nucleon cross section.  
⇒ Mediator mass can not be too large if  $m_\chi < 1$  TeV.
- Collider constraints limit couplings for a reasonable  $m_\phi$  (NP production).
- Constraints from dijet searches prefer  $D_{\lambda,33} \geq D_{\lambda,22}, D_{\lambda,11}$ .
- Direct detection constraints prefer top flavoured DM.
- In combination with the limits on couplings, the RA constraints produce a lower bound for the DM mass (depending on  $m_\phi$ ).
- In SFF the splitting conditions in combination with RA constraints also establishes an upper bound on  $m_\chi$  (depending on  $m_\phi$  and  $\eta$ ).

- All kinds of different constraints → multitude of effects and interesting interplay.
- Especially interesting effect on mixing angle  $\theta_{13}$  due to DD and RA constraints.  
⇒ Future measurements of direct detection experiments can potentially exclude a large class of models.
- Simplified models are powerful tool to study diversity of constraints.
- Going beyond Minimal Flavour Violation is worth the effort.  
→ Dark Minimal Flavour Violation as guidance.

# Thank you!



# Thank you!

# Questions?



Georges Aad et al. “Search for squarks and gluinos with the ATLAS detector in final states with jets and missing transverse momentum using  $\sqrt{s} = 8$  TeV proton–proton collision data”. In: *JHEP* 09 (2014), p. 176. DOI: 10.1007/JHEP09(2014)176. arXiv: 1405.7875 [hep-ex].



Georges Aad et al. “Search for top squark pair production in final states with one isolated lepton, jets, and missing transverse momentum in  $\sqrt{s} = 8$  TeV  $pp$  collisions with the ATLAS detector”. In: *JHEP* 11 (2014), p. 118. DOI: 10.1007/JHEP11(2014)118. arXiv: 1407.0583 [hep-ex].



R Aaij et al. “Precision measurement of D meson mass differences”. In: *JHEP* 1306 (2013), p. 065. DOI: 10.1007/JHEP06(2013)065. arXiv: 1304.6865 [hep-ex].



Prateek Agrawal, Monika Blanke, and Katrin Gemmler. “Flavored dark matter beyond Minimal Flavor Violation”. In: *JHEP* 1410 (2014), p. 72. DOI: 10.1007/JHEP10(2014)072. arXiv: 1405.6709 [hep-ph].






D. S. Akerib et al. “Improved WIMP scattering limits from the LUX experiment”. In: (2015). arXiv: 1512.03506 [astro-ph.CO].



Sinya Aoki et al. “Review of lattice results concerning low-energy particle physics”. In: *Eur.Phys.J. C* 74 (2014), p. 2890. DOI: 10.1140/epjc/s10052-014-2890-7. arXiv: 1310.8555 [hep-lat].



A.J. Bevan et al. “The UTfit collaboration average of D meson mixing data: Winter 2014”. In: *JHEP* 1403 (2014), p. 123. DOI: 10.1007/JHEP03(2014)123. arXiv: 1402.1664 [hep-ph].

-  Monika Blanke et al. “FCNC Processes in the Littlest Higgs Model with T-Parity: a 2009 Look”. In: *Acta Phys.Polon.* B41 (2010), pp. 657–683. arXiv: 0906.5454 [hep-ph].
-  N. Carrasco et al. “ $D^0 - \bar{D}^0$  mixing in the standard model and beyond from  $N_f = 2$  twisted mass QCD”. In: *Phys.Rev.* D90.1 (2014), p. 014502. DOI: 10.1103/PhysRevD.90.014502. arXiv: 1403.7302 [hep-lat].
-  Carlos A. Chavez, Ray F. Cowan, and W.S. Lockman. “Charm meson mixing: An experimental review”. In: *Int.J.Mod.Phys.* A27 (2012), p. 1230019. DOI: 10.1142/S0217751X12300190. arXiv: 1209.5806 [hep-ex].



Csaba Csaki, Adam Falkowski, and Andreas Weiler. “The Flavor of the Composite Pseudo-Goldstone Higgs”. In: *JHEP* 0809 (2008), p. 008. DOI: 10.1088/1126-6708/2008/09/008. arXiv: 0804.1954 [hep-ph].



Yuval Grossman, Yosef Nir, and Gilad Perez. “Testing New Indirect CP Violation”. In: *Phys.Rev.Lett.* 103 (2009), p. 071602. DOI: 10.1103/PhysRevLett.103.071602. arXiv: 0904.0305 [hep-ph].



Alexander L. Kagan and Michael D. Sokoloff. “On Indirect CP Violation and Implications for  $D^0$  - anti- $D^0$  and  $B(s)$  - anti- $B(s)$  mixing”. In: *Phys.Rev.* D80 (2009), p. 076008. DOI: 10.1103/PhysRevD.80.076008. arXiv: 0907.3917 [hep-ph].

# References V



Can Kilic, Matthew D. Klimek, and Jiang-Hao Yu. “Signatures of Top Flavored Dark Matter”. In: *Phys.Rev. D*91.5 (2015), p. 054036. DOI: 10.1103/PhysRevD.91.054036. arXiv: 1501.02202 [hep-ph].



Alexey A Petrov. “Long-distance effects in charm mixing”. In: (2013). arXiv: 1312.5304 [hep-ph].



Gary Steigman, Basudeb Dasgupta, and John F. Beacom. “Precise Relic WIMP Abundance and its Impact on Searches for Dark Matter Annihilation”. In: *Phys.Rev. D*86 (2012), p. 023506. DOI: 10.1103/PhysRevD.86.023506. arXiv: 1204.3622 [hep-ph].



James D. Wells. “Annihilation cross-sections for relic densities in the low velocity limit”. In: (1994). arXiv: hep-ph/9404219 [hep-ph].

# Constraints from SUSY Searches at LHC

[ATLAS collaboration '14]

- Study the process  
 $pp \rightarrow \phi\bar{\phi} \rightarrow q\bar{q}\chi\bar{\chi}$ .
- Depending on decay product of  $\phi$   
we detect either a top signature or  
a jet (+ $\cancel{E}_T$ ).
- Inspiration from SUSY searches at  
LHC  
 $\Rightarrow$  Upper bounds on CS of both  $t\bar{t}$   
and dijet signals.

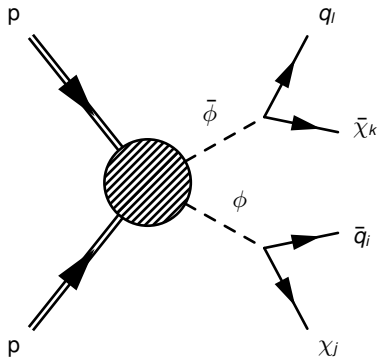
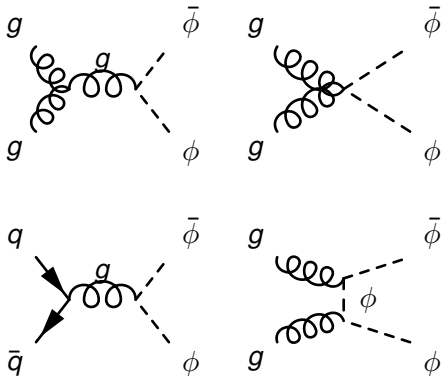


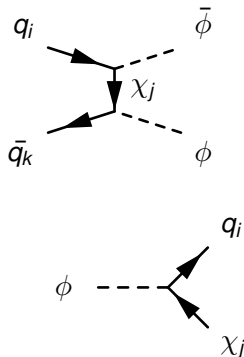
**Figure :** Studied LHC DM production processes.

# Constraints from SUSY Searches at LHC

## Involved QCD processes



## Involved NP processes



## References



- $D_{\lambda,33}$  increased  
→ BR of decay goes up.
- $D_{\lambda,11}, D_{\lambda,22}$  increased  
→ BR of decay goes down.
- **BUT:** For high  $D_{\lambda,11} = D_{\lambda,22}$  we observe increasing excluded areas.

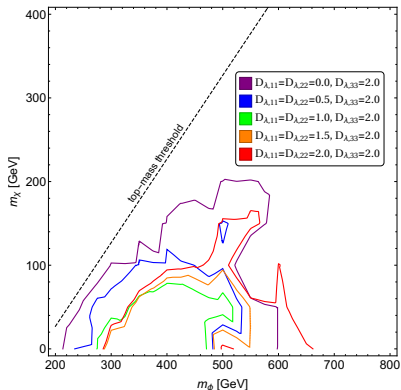


**Figure :** Exclusion plot for  $t\bar{t}$  final state, mixing angles set to zero.

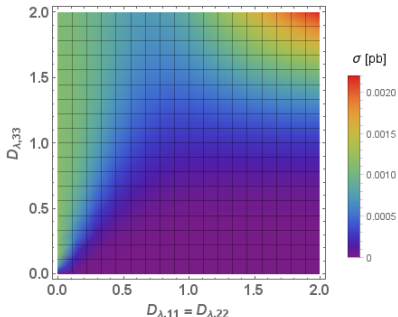


**Figure** : Cross section of  $t\bar{t}$  final state for  $m_\phi = 850$  GeV and  $m_\chi = 50$  GeV, mixing angles set to zero.

## Explanation: NP production

- Major contribution to total production (for high  $D_{\lambda,11}$ ,  $D_{\lambda,22}$ )
- This effect can make up for drop in BR
- $D_{\lambda,33}$  not relevant, since the protons do not contain top
- Very high couplings can lead to serious exclusion areas.

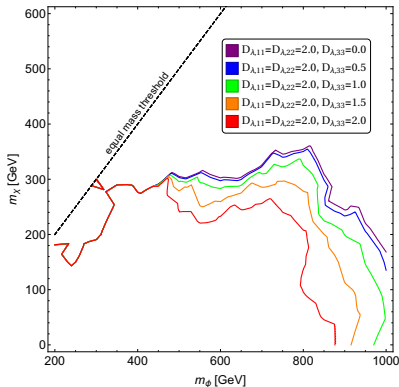


**Figure** : Exclusion plot for dijet final state, mixing angles set to zero.

- Stronger exclusion bounds on model.
- The phenomenologically interesting region is  $m_\chi \leq 1$  TeV.
- Too large couplings  $D_{\lambda,ii}$  would exclude nearly all of parameter space.
- Most serious constraints come from dijet final state.

⇒ Safe parameter space:

$$m_\phi \geq 850 \text{ GeV}$$

$$2.0 \geq D_{\lambda,33} \geq D_{\lambda,22}, D_{\lambda,11}$$

- Mixing angles shift influences between couplings  $D_{\lambda,ii}$ .  
⇒ For big splitting in the couplings, mixing angles can cause big shifts in cross sections.
  - For our choice of  $m_\phi$  bounds from  $t\bar{t}$  final state cause no constraints.
  - Worst allowed case for dijet final state, in our safe parameter space, is  $D_{\lambda,11} = D_{\lambda,22} = D_{\lambda,33} = 2.0$   
⇒ Unchanged by mixing angles.
- ⇒ Mixing angles can cause no problem with this choice of safe parameter space.

# Flavour Constraints from Neutral Meson Mixing

[UTfit collaboration '14]

- No mesons with top quark are possible, the only constraints come from D mesons.  
 $\Rightarrow$  not too strong
- The NP contribution has to be smaller than experimental bounds.

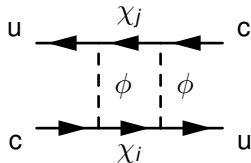


Figure : NP contr. to neutral D meson mixing.

$$\begin{aligned}
 M_{12}^{D, NP} &= \frac{1}{2m_D} \langle \bar{D}^0 | \mathcal{H}_{eff}^{\Delta C=2, new} | D^0 \rangle^* \\
 &= \frac{1}{384\pi^2 m_\phi^2} \sum_{i,j} \lambda_{uj}^* \lambda_{cj} \lambda_{ui}^* \lambda_{ci} \cdot L(x_i, x_j) \cdot \eta_D \cdot m_D f_D^2 \hat{B}_D.
 \end{aligned}$$

# Flavour Constraints from Neutral Meson Mixing

$$\left( (\lambda\lambda^\dagger)_{cu} \right)^2 = \left( (U_\lambda D_\lambda D_\lambda^\dagger U_\lambda^\dagger)_{cu} \right)^2$$

- For degeneracy

$D_{\lambda,11} = D_{\lambda,22} = D_{\lambda,33}$  the mixing matrices  $U_{ij}^\lambda$  will drop out.

- The higher the splitting

$\Delta_{ij} = D_{\lambda,ii} - D_{\lambda,jj}$ , the more we will see the constraints on the mixing angle  $\theta_{ij}$ .

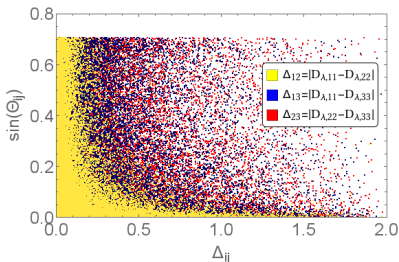


**Figure :** Valid mixing angles for different coupling splittings.  $m_\phi = 850$  GeV and  $m_\chi = 250$  GeV.

$\Rightarrow$  Most significant constraints on  $\theta_{12}$ , other mixings nearly unconstrained.

[Steigman, Dasgupta, Beacom '12]

- Assume DM abundance as a thermal relic,  $T_f \propto \frac{m_\chi}{20}$
- Coannihilation CS has to be just large enough to produce the correct relic density (we allow for a 10% tolerance interval):

$$\langle \sigma v \rangle_{\text{eff,exp}} = 2.2 \times 10^{-26} \text{cm}^3/\text{s}.$$

$\Rightarrow$  cuts out valid area for  $D_{\lambda,ii}$   
depending on  $m_\phi$  and  $m_\chi$

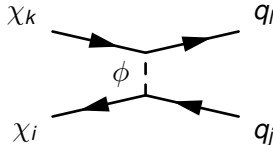


Figure : Coannihilation of DM flavours.

$$\langle \sigma v \rangle_{\text{eff}} = \frac{1}{9} \times \frac{3}{256\pi} \sum_{i,j=1,2,3} \sum_{k,l=u,c,t} \lambda_{ki} \lambda_{ki}^* \lambda_{lj} \lambda_{lj}^* \frac{\sqrt{(4m_\chi^2 - (m_k - m_l)^2)(4m_\chi^2 - (m_k + m_l)^2)}}{\left(m_\phi^2 + m_\chi^2 - \frac{m_k^2}{2} - \frac{m_l^2}{2}\right)^2}.$$

- Depending on the mass splitting of the different DM flavours several freeze out scenarios are possible.

$$m_{ij} = m_\chi (1 + \eta (D_{\lambda,ij})^2 + \dots) \delta_{ij}.$$

- For a DM mass below the top quark mass this decay channel drops out.

⇒ CS formula and hence impact on parameters can be quite different

- Extreme example: only  $\chi_t$  present at freeze out with DM mass below top mass threshold:

$$\langle \sigma v \rangle_{eff} = \frac{3}{256\pi} \sum_{k,l=u,c} \lambda_{k3} \lambda_{k3}^* \lambda_{l3} \lambda_{l3}^* \frac{4m_\chi^2}{(m_\phi^2 + m_\chi^2)^2}.$$



# Quasi Degenerate Freeze Out (QDF) Szenario

- All DM flavours are present at the freeze out.
- We require the mass splitting to be less than 1% (significantly smaller than  $T_f$ ) for this to happen.
- $\eta$  is free parameter  $\rightarrow$  choose it favourable: -0.01.
- This guarantees top flavoured DM (see direct detection section for motivation).
- Constraint cuts out valid area for  $D_{\lambda,ii}$  depending on  $m_\phi$  and  $m_\chi$ .
- Lower bound on  $m_\chi$  due to upper limits for  $D_{\lambda,ii}$ , depending on  $m_\phi$ .

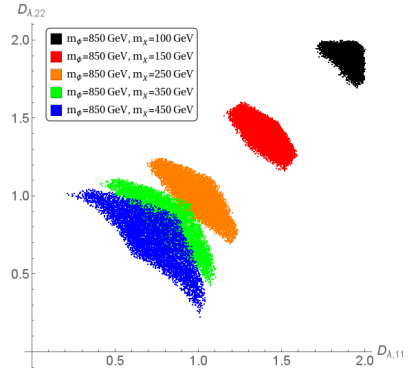


**Figure :** Valid points in quasi degenerate freeze out scenario.

# Single Flavour Freeze Out (SFF) Szenario

- Only  $m_\chi$  present at freeze out.
- We require the mass splitting to be more than 10% (significantly bigger than  $T_f$ ) for this to happen.
- $\eta$  is free parameter  $\rightarrow$  choose it favourable: -0.075.
- This guarantees top flavoured DM (see direct detection section for motivation).
- Constraint cuts out valid area of parameters depending on  $m_\phi$  and  $m_\chi$ , with significant effect on mixing angles.
- In addition to lower bound, we also find an upper bound on  $m_\chi$  due to upper and lower (from mass splitting condition) limits for  $D_{\lambda,ii}$ , depending on  $m_\phi$ .

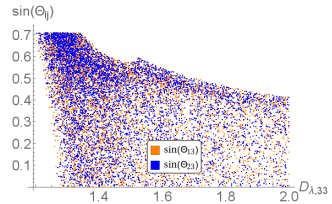


**Figure :** Valid points in single flavour freeze out scenario for  $m_\phi = 850$  GeV and  $m_\chi = 210$  GeV.

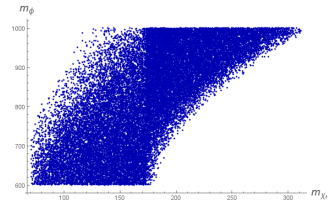
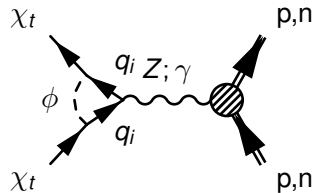
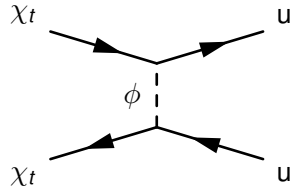
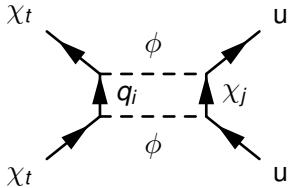


**Figure :** Mass bounds in single flavour freeze out scenario.

# DM Bounds from Direct Detection Experiments

Many contributions to total WIMP-nucleon cross section:

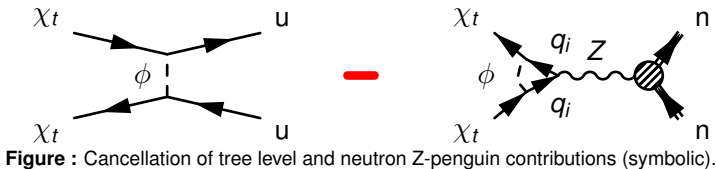
$$\sigma_n^{SI} = \frac{\mu_n^2}{\pi A^2} |Zf_p + (A - Z)f_n|^2.$$



[LUX collaboration '15]

- All contributions have to combine to a WIMP-nucleon cross section below the LUX bounds.
- All contributions are positive, only the Z-penguin with the neutron is negative  
⇒ saves the day.
- Largest contribution comes from tree level process. Largest negative term is hence interference term of tree level and neutron Z-penguin.
- Most important terms, have to nearly cancel each other:

$$A_{II} \cdot D_{\lambda,33}^4 \cdot \sin(\theta_{13})^4 - A_{III} \cdot D_{\lambda,33}^4 \cdot \sin(\theta_{13})^2 \cdot \cos(\theta_{13})^2 \cdot \cos(\theta_{23})^2$$



- Tree level and neutron Z-penguin have to nearly cancel each other.  
⇒ serious constraints on  $\theta_{13}$
- For higher couplings the cancellation gets more complicated.
- For too large couplings the cancellation is no longer possible at all  
→ excluded.
- Top-flavoured DM is the natural choice:  
⇒ Tree level contribution small  
⇒ Neutron Z-penguin contribution large.

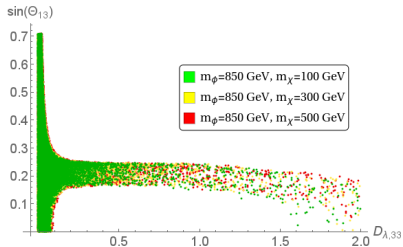
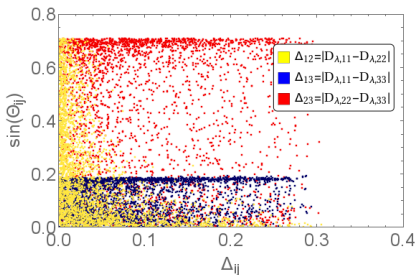


Figure : Valid mixing angle  $\Theta_{13}$  vs  $D_{\lambda,33}$ .

# Combined Analysis of Constraints (QDF)

Combined application of both flavour, relic abundance and direct detection constraint in quasi degenerate freeze out scenario.



**Figure :** Valid points for  $m_\phi = 850$  GeV and  $m_\chi = 150$  GeV (QDF).

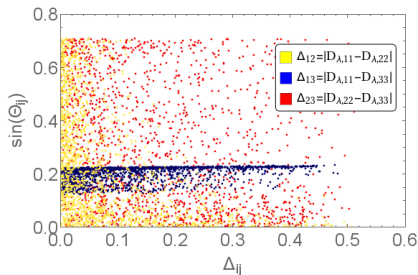


**Figure :** Valid points for  $m_\phi = 850$  GeV and  $m_\chi = 250$  GeV (QDF).

# Combined Analysis of Constraints (QDF)

- A combination of relic abundance and direct detection constraints confine  $\theta_{13}$  to a narrow interval.
- The bounds on the DM mass become more serious, since the parameters do not only have to fulfill relic abundance constraints.
- The combined analysis clearly prefers top flavoured DM.

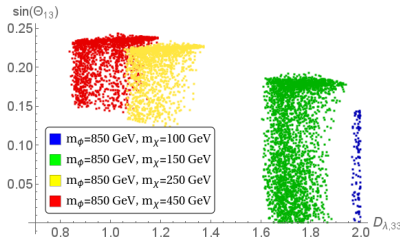
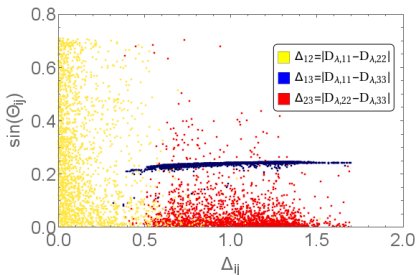


Figure : Valid points in  $\theta_{13}$ - $D_{\lambda,33}$ -plane (QDF).

# Combined Analysis of Constraints (SFF)

Combined application of both flavour, relic abundance and direct detection constraint in single flavour freeze out scenario.



**Figure :** Valid points for  $m_\phi = 850$  GeV and  $m_\chi = 225$  GeV (SFF).

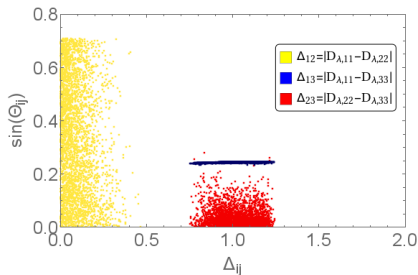


**Figure :** Valid points for  $m_\phi = 850$  GeV and  $m_\chi = 250$  GeV (SFF).



- A combination of relic abundance and direct detection constraints confine  $\theta_{13}$  to a narrow interval (even more serious than in QDF).
- Especially in SFF the combination of all constraints extremely limits the chance of finding a valid configuration of all parameters for  $m_{\chi_t} \leq m_{top}$ .
- The combined analysis clearly prefers top flavoured DM.

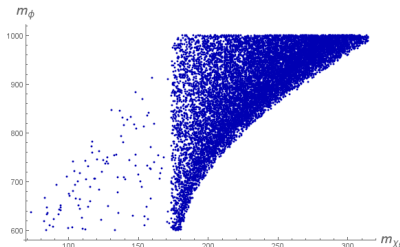


**Figure :** Valid points in mass plot for combined constraints (SFF).

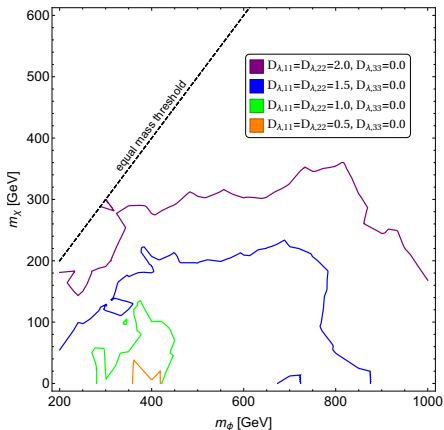


**Figure** : Exclusion plots for dijet final state for various couplings, mixing angles set to zero.

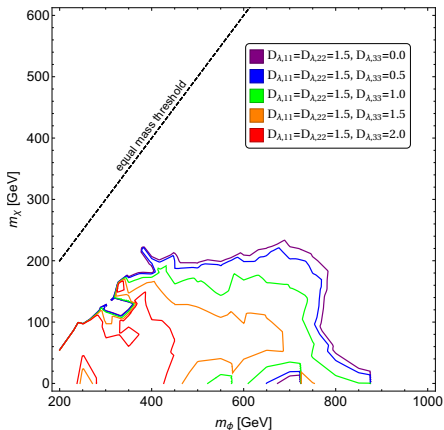


**Figure** : Exclusion plots for dijet final state for various couplings, mixing angles set to zero.

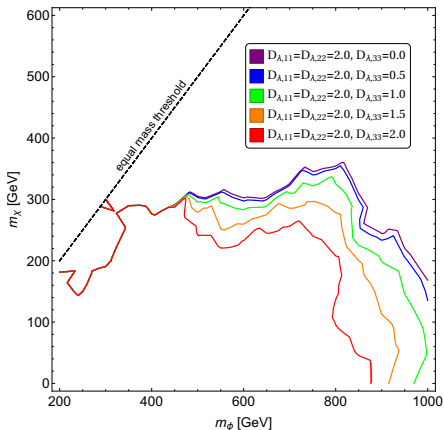


**Figure** : Exclusion plots for dijet final state for various couplings, mixing angles set to zero.

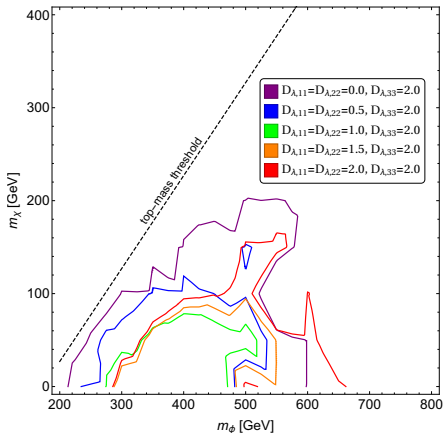


**Figure :** Exclusion plots for  $t\bar{t}$  final state for various couplings, mixing angles set to zero.

# Backup Material 5

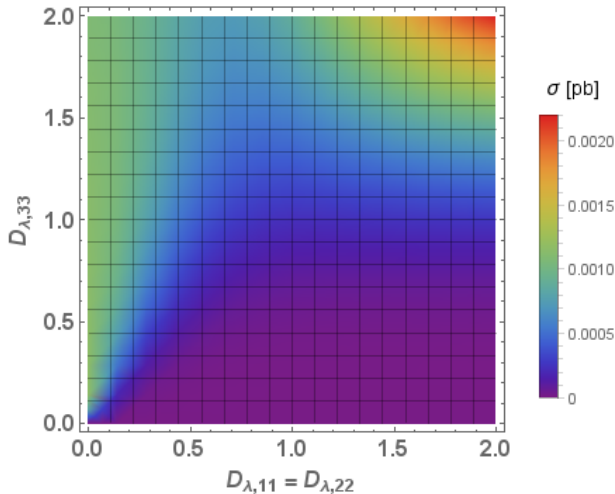


**Figure** : Cross section for  $t\bar{t}$  final state, mixing angles set to zero.

relative number of valid points

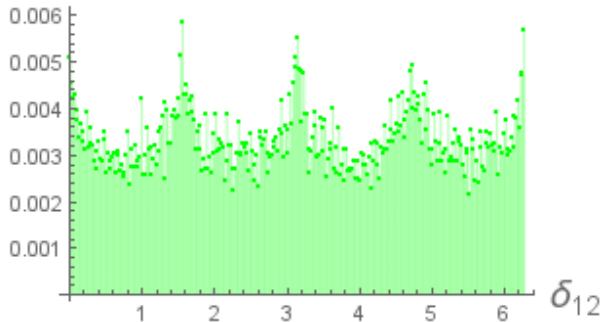
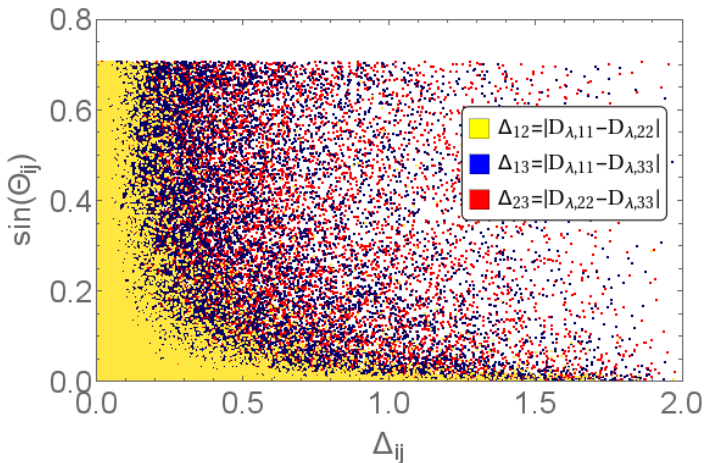
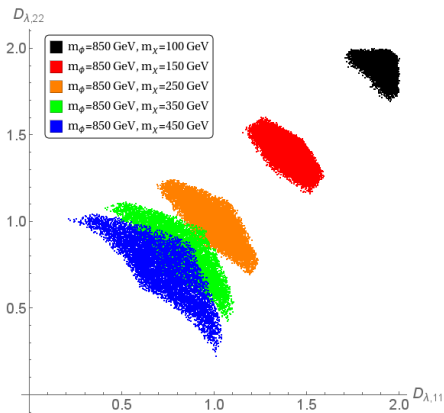


Figure : Impact of flavour constraints on  $\Theta_{12}$ .



**Figure :** Valid mixing angles for different coupling splittings.  $m_\phi = 850$  GeV and  $m_\chi = 250$  GeV.





**Figure** : Valid points in quasi degenerate freeze out scenario in  $D_{\lambda,11} - D_{\lambda,22}$ -plane for various DM masses.

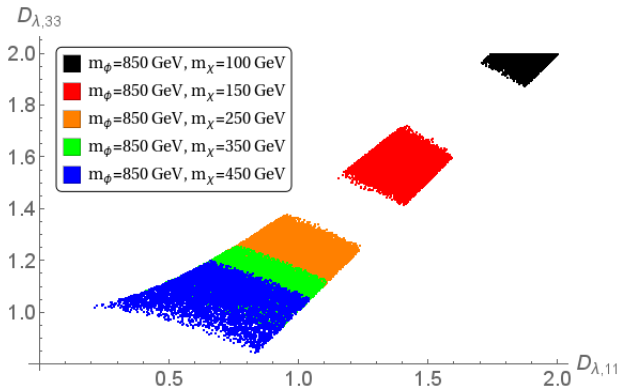


**Figure** : Valid points in quasi degenerate freeze out scenario in  $D_{\lambda,11} - D_{\lambda,33}$ -plane for various DM masses.

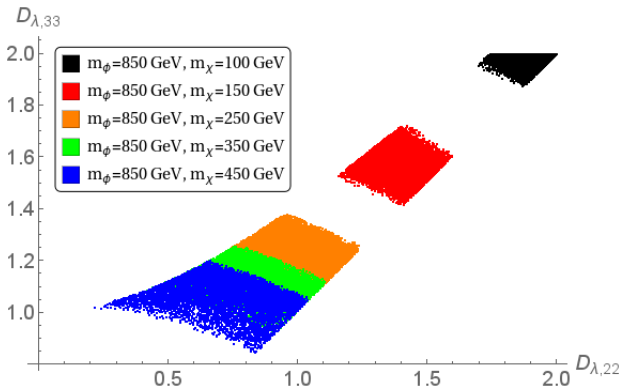


**Figure :** Valid points in quasi degenerate freeze out scenario in  $D_{\lambda,22} - D_{\lambda,33}$ -plane for various DM masses.

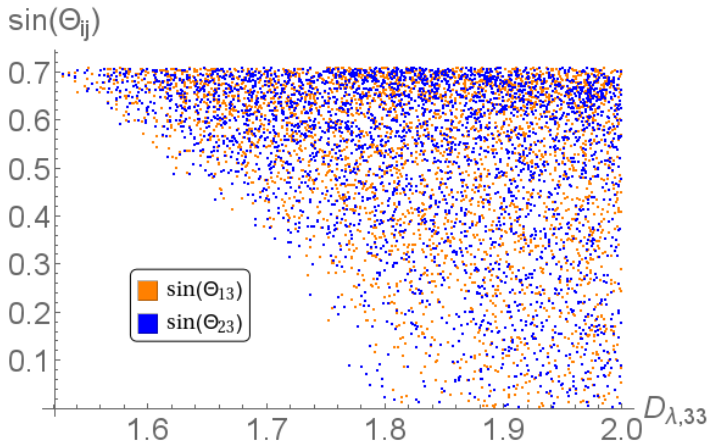


**Figure** : Valid points in single flavour freeze out scenario in  $D_{\lambda,33} - \sin(\Theta_{ij})$ -plane for  $m_\phi = 850$  GeV and  $m_\chi = 150$  GeV.

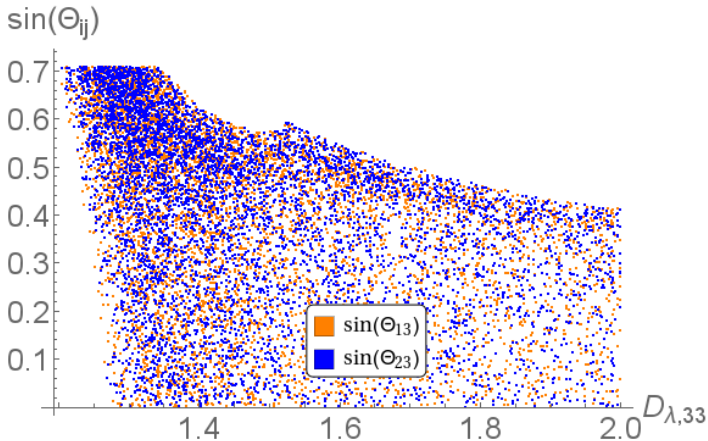


**Figure :** Valid points in single flavour freeze out scenario in  $D_{\lambda,33} - \sin(\Theta_{ij})$ -plane for  $m_\phi = 850$  GeV and  $m_\chi = 210$  GeV.

# Backup Material 13

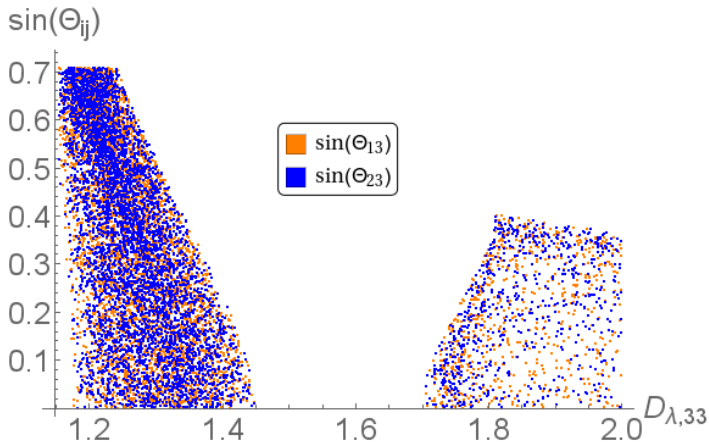


**Figure** : Valid points in single flavour freeze out scenario in  $D_{\lambda,33} - \sin(\Theta_{ij})$ -plane for  $m_\phi = 850$  GeV and  $m_\chi = 230$  GeV.

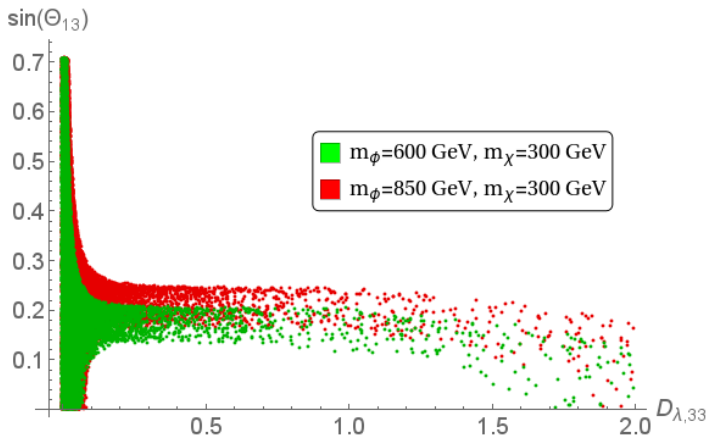


**Figure :** Valid points for LUX bounds in  $D_{\lambda,33} - \sin(\Theta_{13})$ -plane.

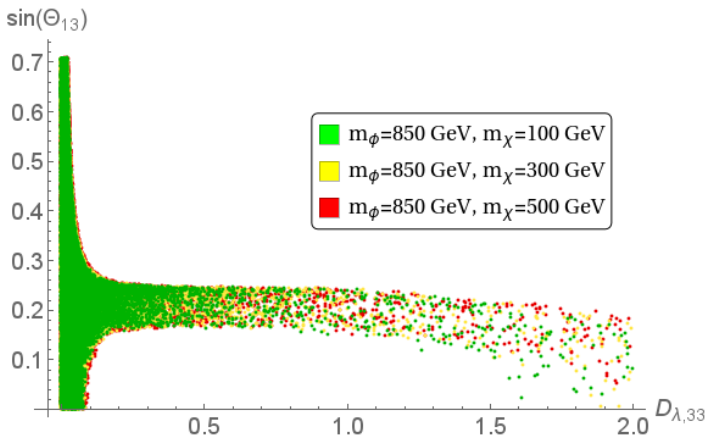


**Figure :** Valid points for LUX bounds in  $D_{\lambda,33} - \sin(\Theta_{13})$ -plane.



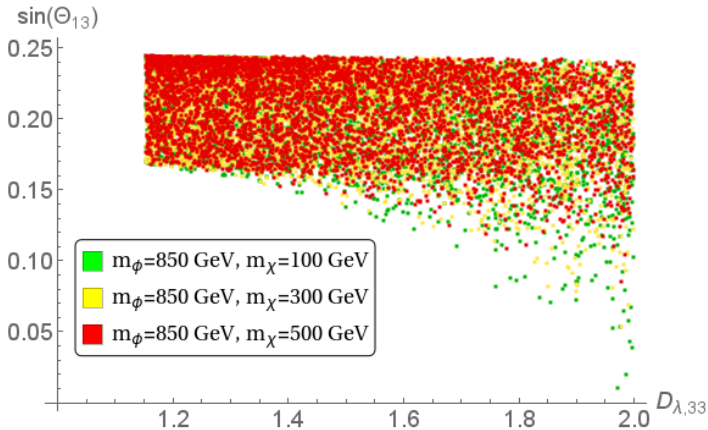


**Figure :** Valid points for LUX bounds in  $D_{\lambda,33} - \sin(\Theta_{13})$ -plane, with SFF splitting applied.

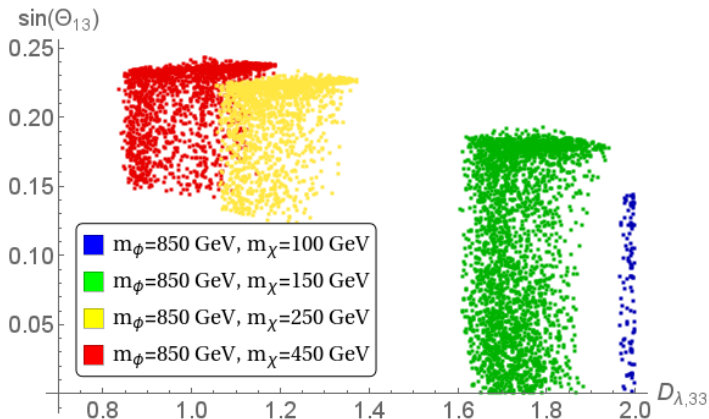


**Figure :** Valid points of combined analysis for quasi degenerate freeze out scenario in  $D_{\lambda,33} - \sin(\Theta_{13})$ -plane for different DM masses.

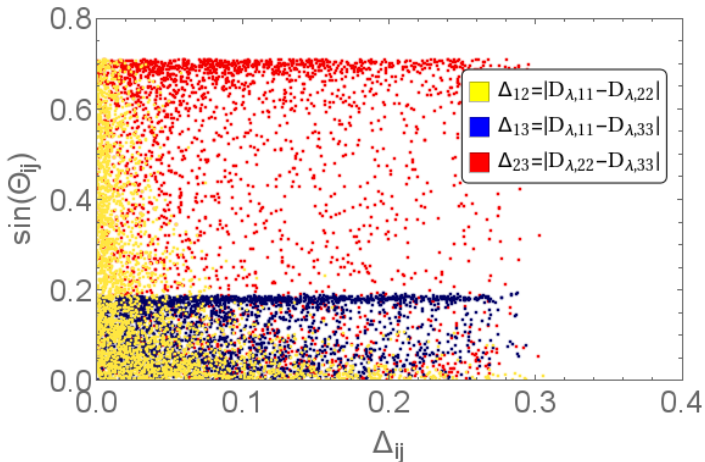


**Figure :** Valid mixing angles for different coupling splittings for quasi degenerate freeze out scenario.  $m_\phi = 850$  GeV and  $m_\chi = 150$  GeV.

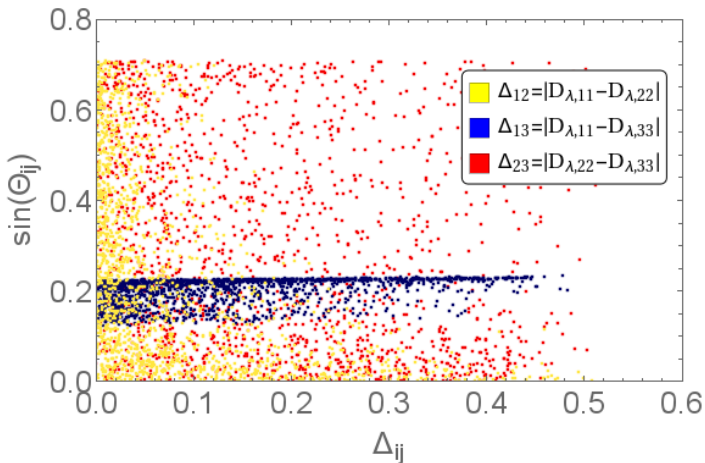


**Figure :** Valid mixing angles for different coupling splittings for quasi degenerate freeze out scenario.  
 $m_\phi = 850$  GeV and  $m_\chi = 250$  GeV.

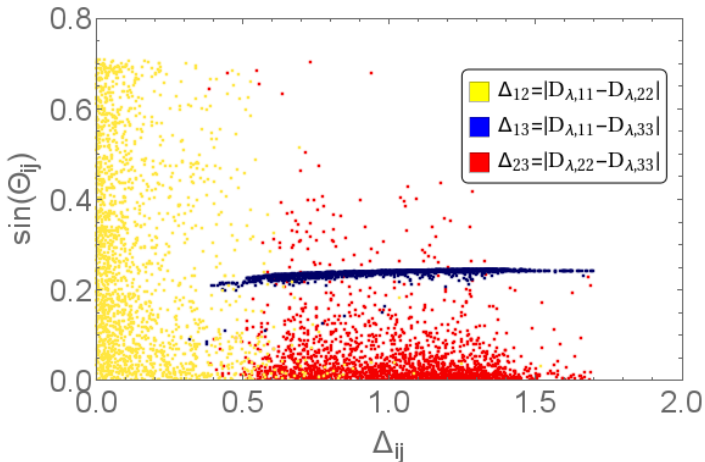


**Figure :** Valid mixing angles for different coupling splittings for single flavour freeze out scenario.  
 $m_\phi = 850$  GeV and  $m_\chi = 225$  GeV.

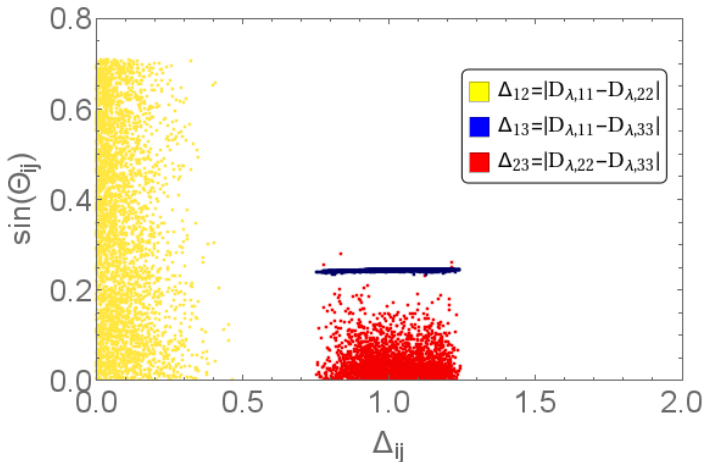


**Figure :** Valid mixing angles for different coupling splittings for single flavour freeze out scenario.  
 $m_\phi = 850$  GeV and  $m_\chi = 250$  GeV.